formation of two neutral species **4** and **7** which will recombine less easily in dilute THF on the other hand, so that the persistence of the spectrum of **1** in THF would be rather unexpected.

Finally, the titanocene cation was found by X-ray studies to be associated with one molecule of DME in the structure of $(Cp_2Ti\cdot DME)_2Zn_2Cl_6\cdot C_6H_6$.[5] It is also formed by dissolution of $(Cp_2TiCl)_2$ in water.[8] Its possible existence in THF, as we tried

to demonstrate in this work, is then not unusual.

Further studies by ESR on the species formed in solutions containing titanocene (III) compounds is currently in progress.

A New Type of Transition-Metal Dimer Based on a Hexaphosphine Ligand System: $Co_2(CO)_4(eHTP)^{2+}$ (eHTP = $(Et_2PCH_2CH_2)_2PCH_2P(CH_2CH_2PEt_2)_2$)

Fredric R. Askham,[†] **George G. Stanley,***[†] **and Edward C. Marques**[‡]

Contribution from the Department of Chemistry, Washington University, St. Louis, Missouri 63130, and the Physical Sciences Center, Monsanto Company, St. Louis, Missouri 63166. Received April 15, 1985

Abstract: The synthesis and characterization of a new hexa-*tert*-phosphine ligand system, $(Et_2PCH_2CH_2)_2PCH_2P(CH_2CH_2PEt_2)_2$, **1**, is described. This ligand has the ability to both tris-chelate and bridge two transition metals, either in a closed-mode, M–M bonding geometry, or in an open-mode configuration in which the two metal atoms are 6–7 Å apart. Reaction of **1** with 2 equiv of $CoCl_2$ initially produces, in high yields, the paramagnetic, binuclear, red–brown Co(II) compound, $Co_2Cl_4(eHTP)$, **4**, where eHTP = **1**. An Extended X-ray Absorption Fine Structure (EXAFS) spectrum of **4** shows Co–P and Co–Cl bond distances in the 2.2–2.4-Å region and no Co–Co contact distance less than 4.0 Å, indicating that **4** is in an open-mode geometry. On standing, **4** dissociates two chloride ligands to form the green, paramagnetic $Co_2Cl_2(eHTP)^{2+}$ complex, **5**, which precipitates out of the reaction mixture, either as the chloride or, if an extra equivalent of $CoCl_2$ is used, the $CoCl_4^{2-}$ salt. The EXAFS spectrum on the $CoCl_4^{2-}$ salt of **5** is very similar to that of **4**, indicating that **5** is also in an open-mode geometry. Reaction of **4** or **5** (alone or mixed) with H_2/CO (33% CO) and an extra equivalent of $CoCl_2$ at 50 bar and 80 °C forms, in high yields, the yellow-green, diamagnetic Co(I) binuclear carbonyl/eHTP complex, $[Co_2(CO)_4(eHTP)^{2+}][CoCl_4^{2-}]$, **6a**, which can be metathesized with aqueous $NaPF_6$ to give the yellow PF_6^- salt, **6b**. **6** has been characterized by ^1H and ^{31}P NMR, EXAFS, mass spectroscopy, IR, and a crystal structure. Crystals of **6b** belong to the monoclinic space group $C2/c$, with unit cell parameters $a = 26.464$ (4) Å, $b = 12.562$ (2) Å, $c = 14.380$ (3) Å, $\beta = 99.04$ (1)°, $V = 4721$ (3) Å^3, and $Z = 4$. The structure was refined to give $R = 0.070$ and $R_w = 0.106$. The molecule lies on a 2-fold axis, passing through the bridging methylene group of the eHTP ligand. The complex has the central bis(phosphino)methane portion of the eHTP ligand adopting a unique inverted coordination geometry to give an open-mode complex with the two cobalt atoms separated by 6.697 (1) Å. The cobalt atoms have a distorted trigonal-bipyramidal geometry with one carbonyl ligand and two terminal phosphorus atoms of the eHTP ligand in the equatorial plane.

Despite the large amount of interest in utilizing transition-metal dimers and clusters as homogeneous catalysts, few such systems have been discovered,[1] while even fewer have been demonstrated to be more effective than mononuclear systems already known. Two major problems traditionally associated with research into polynuclear complexes have been difficulties in synthesizing new species in a stepwise and rational fashion and the often ready fragmentation of these polynuclear systems into mononuclear complexes which can lead to confusion about the nature of the reactive species in solution.

In the last few years, however, there has been an increasing amount of work directed at solving these problems. Stone,[2] Osborn,[3] and Vahrenkamp,[4] for example, have developed a variety of elegant synthetic routes for preparing homo- and heterometallic clusters. The general strategy in each of these methods has been to use a ligand system that cannot only act as a template for building up a cluster in a stepwise synthesis but has also been designed to have the proper geometric and steric factors needed to constrain the metal centers in proximity, even in the event of M–M bond-breaking reactions which often lead to fragmentation.

The fragmentation of polynuclear systems is a particularly severe problem when dealing with medium-to-high-pressure carbon monoxide reaction conditions, as found in the homogeneously

catalyzed ethylene glycol process,[5] or in studying the potentials for photocatalysis. An ideal type of ligand system would be one which cannot only bridge two or more metal atoms, but also chelates the metal centers in some way to give a polynuclear complex which is extremely resistant to M–M *and* M–L-induced fragmentation reactions.

We have decided to start with the simplest of cluster systems, i.e., transition-metal dimers, and would like, therefore, to report the design and synthesis of a new hexaphosphine ligand system for the assembly of binuclear complexes and the structural characterization of a novel open-mode dicobalt carbonyl complex based on this ligand system.

(1) (a) Muetterties, E. L.; Krause, M. J. *Angew. Chem., Int. Ed. Engl.* **1983**, *22*, 135. (b) Johnson, B. F. G. "Transition Metal Clusters"; Wiley: New York, 1980; p 545.

(2) (a) Chetcuti, M.; Green, M.; Howard, J. A. K.; Jeffrey, J. C.; Mills, R. M.; Pain, G. N.; Porter, S. J.; Stone, F. G. A.; Wilson, A. A.; Woodward, P. *J. Chem. Soc., Chem. Commun.* **1980**, 1057. (b) Stone, F. G. A. In "Inorganic Chemistry Toward the 21st Century"; Chisholm, M. H., Ed.; ACS: Washington D.C., 1983; ACS Symp. Ser. No. 211, p 383. (c) Stone, F. G. A. *Angew. Chem., Int. Ed. Engl.* **1984**, *23*, 89.

(3) (a) Osborn, J. A.; Stanley, G. G. *Angew. Chem., Int. Ed. Engl.* **1980**, *19*, 1025. (b) Bahsoun, A. A.; Osborn, J. A.; Voelker, C. *Organometallics* **1982**, *1*, 1114.

(4) (a) Vahrenkamp, H.; Fischer, K.; Muller, M. *Angew. Chem., Int. Ed. Engl.* **1984**, *23*, 140. (b) Richter, F.; Vahrenkamp, H. *Ibid.* **1979**, *18*, 531.

(5) (a) Keim, W.; Berger, M.; Eisenbeis, A.; Kadelka, J. *J. Mol. Catal.* **1981**, *13*, 95. (b) Knifton, J. F. *J. Chem. Soc., Chem. Commun.* **1983**, 729.

[†] Washington University.
[‡] Monsanto Co.

Experimental Section

General Procedures. Under inert atmosphere, CH_2Cl_2 was distilled from CaH_2, methanol and ethanol were distilled from magnesium, and all other solvents were distilled from sodium benzophenone ketyl. All manipulations, unless otherwise noted, were carried out under inert atmosphere by using glovebox or standard Schlenk line techniques. 2,2'-Azobis(isobutyronitrile) was obtained from Pfaltz & Bauer and recrystallized from methanol. Et_2PCl was obtained from Strem Chemicals and used as received. Me_3SiCl, methyllithium, and vinylmagnesium bromide were purchased from Aldrich and used without further purification. White phosphorus and sodium, potassium, and anhydrous $CoCl_2$ were obtained from the Alfa Division of Morton Thiokol.

A Berghof Teflon-lined 250-mL laboratory autoclave was used for high-pressure runs. High-purity CO/H_2 gas mixture (33.4% CO) from Matheson was used as received for the autoclave runs. ^1H and ^{31}P NMR spectra were run on a JEOL FX-100 spectrometer. Infrared spectra were run on a Perkin-Elmer Model 283B spectrometer. NMR simulations were done on a Bruker Aspect 2000 stand-alone data processing computer system. Mass spectra were run on a Finigan 3200 instrument equipped with a fast atom bombardment (FAB) source. Elemental analyses were performed by Galbraith Laboratories, Inc., Knoxville, TN.

Although some of the following procedures for the ligand synthesis have been reported, we have made a number of modifications in the preparations and, therefore, report them here in detail.

$P(SiMe_3)_3$.[6] White phosphorus (22.8 g, 0.736 mol) was cut under water, quickly transferred to a 2000-mL two-neck flask equipped with a reflux condenser and previously purged with N_2 or argon and then dried by vacuum for 4 h. Dimethoxyethane (1700 mL) was then added under inert atmosphere and a high-torque mechanical stirrer inserted. Sodium–potassium alloy (78 g, 2.4 mol), prepared from a 60.5 g of potassium/26.8 g of sodium mixture, was syringed into the vigorously stirred solution over 15 min. The solution darkened and warmed spontaneously. Heat was then applied to achieve reflux and maintained for 24 h. To the black refluxing solution, neat degassed chlorotrimethylsilane (340 mL, 2.68 mol) was added slowly. A vigorous reaction occurred, thickening the reaction mixture with sodium and potassium chloride after 150–200 mL of Me_3SiCl had been added. At the end of the addition, the reaction mixture was grey and quite thick. It is *very* important that good stirring be maintained; otherwise the yield of $P(SiMe_3)_3$ will be lowered. This mixture was refluxed for 3 days.

After cooling, the reaction mixture was filtered either through a 1000-mL Schlenk frit (available from Aldrich) or through a large Buchner funnel in a glovebox, and the salt was washed with several portions of hexane. Note that the salt waste usually catches fire on exposure to the atmosphere so appropriate precautions should be taken when discarding it. The hexane washings were combined with the filtrate and vacuum-evaporated (1 torr) at room temperature until no further evaporation occurred. Distillation of the residue at 0.5–1.0 torr gave 134 g (73% yield) of clear colorless liquid $P(SiMe_3)_3$ (bp 54–57 °C) [lit. yield = 60–75%]. $P(SiMe_3)_3$ is pyrophoric and must be handled under inert atmosphere.

$(Me_3Si)_2PCH_2P(SiMe_3)_2$.[7] $P(SiMe_3)_3$ (69.0 g, 0.276 mol) was diluted with 325 mL of THF and cooled in an ice bath to 0 °C. One equivalent of methyllithium (178 mL of 1.56 M solution in diethyl ether, 0.276 mol) was added over a 30-min period. The solution turned a clear yellow after the addition of the first few drops of MeLi, and this color persisted but did not darken further upon addition of the remaining MeLi solution. This was allowed to stir and warm slowly to room temperature overnight. All volatiles were removed by vacuum, leaving, at first, a light yellow solid. Pumping was continued until all the yellow color had disappeared. This white solid was then mostly dissolved in 600 mL of hexane and the suspension added dropwise via a cannula to CH_2Cl_2 (10 mL, 0.16 mol) in 100 mL of hexane. Precipitation of a white solid occurred soon after the addition had started. Addition was complete after 5 h and stirring continued overnight.

The solution was concentrated, filtered, and distilled under vacuum (0.5 torr). Clear colorless $(Me_3Si)_2PCH_2P(SiMe_3)_2$ (46 g, 91% yield) was collected at 105–112 °C.

$Et_2P(CH=CH_2)$.[8,9] A 1.3 M THF solution (250 mL) of vinylmagnesium bromide was cooled to 0 °C in a 1000-mL flask covered with aluminum foil to prevent exposure to light. To this solution, chlorodiethylphosphine (29.7 g, 0.239 mol) in 300 mL of THF was added slowly. The solution was allowed to warm gradually overnight and then stirred
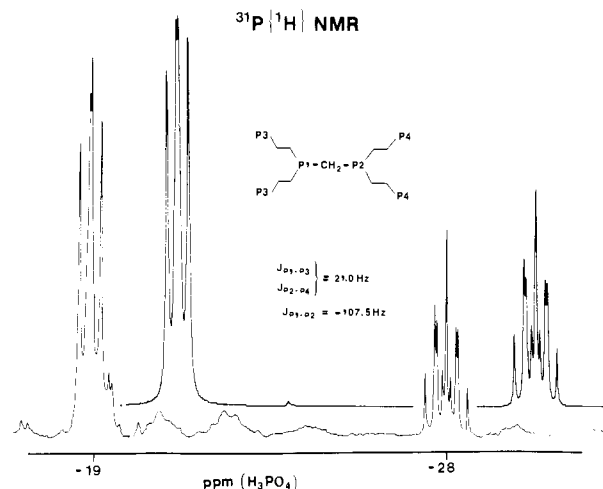
(6) Becker, G.; Holderich, W. *Chem. Ber.* **1975**, *108*, 2484.
(7) Fritz, V. G.; Holderich, W. *Z. Anorg. Allg. Chem.* **1977**, *431*, 76.
(8) (a) Foster, D. J. Brit. Patent 870 425, 1961. (b) *Chem. Abstr.* **1961**, *55*, 24566i.
(9) Baban, J. A.; Cooksey, C. J.; Roberts, B. P. *J. Chem. Soc., Perkin Trans. 2* **1979**, 781.

Figure 1. $^{31}P\{^1H\}$ NMR of $(Et_2PCH_2CH_2)_2PCH_2P(CH_2CH_2PEt_2)_2$. Experimental spectrum on bottom, and simulated spectrum on top (offset). The spectrum is an $A_2XX'A_2'$-type spin system with the four chemically equivalent terminal phosphorus atoms forming the downfield, pseudotriplet pattern and the two central chemically equivalent phosphorus atoms forming the upfield, pseudoquintet pattern. The coupling constants used in the simulation are listed in the figure.

for an additional 24 h. Hydrolysis of the cooled reaction mixture with degassed saturated aqueous ammonium chloride solution (200 mL) was followed by removal of the organic layer by cannula. The remaining aqueous layer was washed with two 50-mL portions of diethyl ether which were then combined with the organic layer and dried with sodium sulfate. The filtered organic layer was distilled at ambient pressure under inert atmosphere to give 22 g (79% yield) of clear colorless $Et_2P(CH=CH_2)$ (bp 124–127 °C). Alternatively, the hydrolysis step could be avoided by trap to trap vacuum distillation of all volatiles from the reaction mixture followed by fractional distillation as before. ^{31}P NMR of the crude reaction mixture, however, indicates that the reaction is almost quantitative: ^1H NMR δ complex pattern for ethyl groups with major peaks at 1.16, 1.26, 1.38, 1.47, 1.64, 1.74, and 1.79, another complex pattern for the vinylic protons with at least 14 peaks between 5.44 and 6.6; ^{31}P NMR δ (H_3PO_4) −21.2 (s).

$(Et_2PCH_2CH_2)_2PCH_2P(CH_2CH_2PEt_2)_2$, **1** (eHTP). $(Me_3Si)_2PCH_2P(SiMe_3)_2$ (20 g, 0.054 mol) was diluted in 50 mL of cyclohexane. Four equivalents of methanol (8.8 mL, 0.217 mol) was injected neat into the stirred solution which warmed but was not permitted to reflux (cool water bath). The reaction was then allowed to stir overnight. Diethylvinylphosphine (25.3 g, 0.218 mol) was injected neat into the solution followed by the addition of dry 2,2'-azobis(isobutyronitrile) (AIBN, 0.25 g, 1.52 mmol). A reflux condenser was then attached and the solution refluxed overnight.

All solvent was vacuum-evaporated, and the yellow oil that remained was heated at 100 °C and 1 torr for 4 h. Column chromatography (short column) on neutral alumina with diethyl ether followed by vacuum evaporation of the solvent left a clear, colorless, nonvolatile oil, yield 75–85%. The ligand could also be distilled (205 °C at 0.15 torr) to give slightly lower yields.

Elemental analysis was not run since there were still traces of an unidentified impurity present. Close examination of the ^1H and ^{31}P NMR spectra for impurity peaks, however, indicated that the product was at least 98% pure, either from column chromatography or distillation. The FAB mass spectrum of **1** showed a parent peak at 544 as well as the characteristic M − 1 and M + 1 peaks from the FAB technique.

^1H NMR δ (C_7D_8, 100 MHz) overlapping pattern with peaks at 0.88, 0.98, 1.13, 1.20 (major peak), 1.32 and 1.48; ^{31}P NMR (acetone-d_6, δ 40.48 MHz) (H_3PO_4) −19.3 (pseudo-triplet, 4 P), −28.2 (pseudo-quintet, 2 P); IR (neat) 2960, 2930–2880 (vs), 2820 (m), 1460 (s), 1420 (s), 1380 (s), 1265 (sh), 1240 (m), 1170 (m), 1100,−1085 (m,br), 1040 (ms), 980 (mw), 870 (w, br), 840 (sh), 760 (s, br), 700 (sh) cm^{-1}. Copies of the ^1H NMR and infrared spectrum are included in the supplementary material.

^{31}P **NMR Simulation of 1.** Bruker program PANIC was used to manually model the experimental spectrum. A four-spin phosphorus system was used, with the two-center phosphorus atoms (P1, P2) having the same upfield chemical shift and the four terminal phosphorus atoms (P3, P4) being assigned the same downfield shift, both of which were based on the center of the experimental patterns (see Figure 1). The P1,2–P3,4 coupling was readily determined from the experimental spectrum and set

at 21.0 Hz. The P1–P2 coupling, though not obvious, was easily established via the simulation program.

Initially only positive coupling constants were assumed, but it was found that the intensity pattern of the triplet could not be properly modeled. Changing the sign of the P1–P2 coupling constant resulted in a much improved fit of the intensity pattern. The line widths of the two patterns are also quite different: the four terminal phosphorus atoms have a line width of 2.8–2.9 Hz, while the two central phosphorus atoms have a line width of only 1.7 Hz. Since only a single line width could be used for the simulation, two simulations were run using line widths of 2.9 and 1.7 Hz. These were cut and pasted together to give the final simulation shown in Figure 1.

The final coupling constants from the simulation are as follows: P1–P2 = –107.5 Hz and P1–P3, P2–P4 = 21.0 Hz; intensities calcd (exptl) pseudo-triplet = 0.86 (0.77), 0.99 (0.91), 1.00 (1.00), 0.94 (0.84); pseudo-quintet (separately normalized) = 0.33 (0.30), 0.69 (0.63), 0.59 (0.57), 0.37 (0.32), 1.00 (1.00), 0.35 (0.29), 0.58 (0.53), 0.57 (0.52), 0.26 (0.24); peak splittings, left to right (Hz) calcd (exptl) pseudo-triplet = 9.54 (9.52), 1.85 (1.95), 9.46 (9.52); pseudo-quintet = 9.40 (9.52), 2.02 (2.20), 5.32 (5.37), 4.08 (3.91), 4.08 (4.15), 5.38 (5.37), 1.93 (1.95), 9.46 (9.52).

$Co_2(CO)_4(eHTP)^{2+}$, **6a and 6b.** eHTP (0.300 g, 0.551 mmol) was diluted with 100 mL of ethanol. Anhydrous $CoCl_2$ (0.215 g, 1.654 mmol, 3 equiv) was dissolved in 50 mL of ethanol and then added dropwise via a stainless-steel cannula to the magnetically stirred eHTP solution. The solution immediately turned yellow and darkened to reddish-brown as the addition proceeded. The solution remained homogeneous until approximately 30 mL of the $CoCl_2$ solution had been added. Further $CoCl_2$ addition caused the precipitation of a fine green solid. On standing, the red–brown solution continued to deposit green precipitate until the red–brown solution color disappeared. If the reaction is conducted in THF, however, the red–brown species is stabilized to a certain extent and will remain in solution.

After the addition was completed, the entire reaction mixture was transferred to a 250-mL laboratory autoclave in a glovebox, sealed, and removed. The autoclave was charged with CO/H_2 (33.4% CO) to 50 bar and heated to 80 °C for 12–36 h (the time is not particularly critical).

After cooling, the autoclave was depressurized and the green suspension transferred to a 250-mL flask and vacuum-evaporated to give 0.53 g of $Co_2(CO)_4(eHTP)\cdot CoCl_4$, **6a** (98% yield). This material is air-stable in the solid state for a period of months. Solutions are slightly air-sensitive, with noticeable decomposition occurring after only a few days. It is sparingly soluble in polar organic solvents such as THF, acetonitrile, ethanol, methanol, etc. It is very soluble in H_2O.

6a (0.68 mmol, 0.53 g) was dissolved in 12 mL of water (degassing is not necessary, but recommended) to give an orange solution which was filtered through Celite. $NaPF_6$ (0.515 g, 3.07 mmol) in 3 mL of water was added dropwise to the orange $Co_2(CO)_4(eHTP)^{2+}$ solution, causing the immediate precipitation of a light-yellow solid. The solution was cooled to 0 °C and vacuum-filtered. The light-yellow solid was washed with three 10-mL portions of cold water and then dried in a vacuum desiccator to give 0.533 g of $Co_2(CO)_4(eHTP)\cdot 2PF_6$, **6b** (91% yield). Recrystallization by slowly evaporating a solution in acetone/ethanol/H_2O yields large yellow crystals. **6b** is soluble in polar organic solvents such as THF, ethanol, methanol, acetonitrile, and acetone. It is insoluble in H_2O and nonpolar organic solvents.

Anal. Calcd for $C_{29}H_{59}Co_2F_{12}O_{4.5}P_8$ ($^1/_2 H_2O$ of crystallization from X-ray structure): C, 32.43; H, 5.54; P, 23.09. Found: C, 31.83; H, 5.28; P, 22.51. IR (KBr) ν_{CO} 2019 and 1968 cm⁻¹; ¹H NMR (acetone-d_6) δ 1.05–1.43 (multiplet), 2.2 and 2.7 (broad peaks), 3.1 (t, bridging CH_2, J_{P-H} = 8 Hz); ³¹P NMR (acetone-d_6) δ (H_3PO_4) 127.2 (quin, 2 P, J_{P-P} = 35 Hz), 83.4 (d, 4 P, J_{P-P} = 47.6 Hz), –143.7 (heptet, J_{P-F} = 708 Hz). Copies of the full IR and ¹H and ³¹P NMR are included as supplementary information.

Extended X-ray Absorption Fine Structure Spectroscopy (EXAFS). Data was collected on an in-house laboratory instrument in the Physical Sciences Center at Monsanto Co., St. Louis, MO. The instrument uses a 15-kW rotating silver anode X-ray source (Elliot Model GX-21) and a 20-cm fixed radius Rowland circle spectrometer.[10] The spectrometer design uses a cylindrically bent single crystal as a monochromator for the focused X-ray beam. For our application in the region of the Co 1s absorption edge (7.709 keV), a Si ⟨311⟩ crystal was used. Linear source dimensions of 1 cm × 0.125 mm were obtained through a photographic pinhole image, and a spectrometer resolution of 7 eV was estimated by using the measured and natural widths of the tungsten Lβ emission lines.[11] Gas proportional detectors were set up in a transmission mode of constant incident intensity with feedback control of the generator current. At energies up to 15 eV above the absorption threshold, data points were recorded in steps of constant photoelectron wavenumber.

Samples for the EXAFS experiments were prepared by mixing a small amount of Apiezon M grease into the powdered sample under inert atmosphere. The powder/grease mixture was pressed between two sheets of 0.10 mil Mylar X-ray film using standard glass microscope slides. Absorption was optimized by adjusting the thickness of the sample as monitored by testing in the X-ray beam. $CoCl_2$ and $[Co(\eta^5\text{-pentadie-nyl})(PEt_3)_2][BF_4]$[12] were used as reference samples to check the position of the Co absorption edge and to determine carbon, phosphorus, and chlorine atom scattering factor phase shifts.

In processing the EXAFS data, the monotonic X-ray absorption ("atomic"-like absorption and Compton background) was subtracted using a multiregion polynomial spline method.[13] Residual modulations were normalized to one atom absorption by using McMasters energy-dependent photoabsorption cross sections.[14] The functional form of the normalized oscillating absorption component, $\chi(k)$, is given by:

$$\chi(k) = \sum_i \left(\frac{N_i}{kr_i^2} \right) e^{-2k\sigma_i^2} e^{-2r_i/\lambda_i(k)} B_i(k) \sin(2kr_i + \Phi_i(k))$$

where $\sum_i$ represents a superposition over various single scattering shell vectors in the structure. Each shell i has N_i = coordination number, r_i = average bond distance, and σ_i^2 = mean squared relative displacement (thermal motion, disorder parameter). The EXAFS function includes elastic back-scattering amplitude, $B_i(k)$, and phase shift, $\Phi_i(k)$, for each shell, as well as an electron mean free path term $\lambda_i(k)$.[15]

Fourier transforms of this corrected data yield radial transform functions with peaks at positions in radius (which must be subsequently corrected for the respective atomic scattering factor phase shifts) from the absorbing cobalt atom. A low-pass Fourier transform filter was applied in order to isolate the EXAFS modulations arising from photoelectron back-scattering from neighboring atoms within a short sphere of radius, enhancing the data from the first coordination sphere about the cobalt atom.

X-ray Crystallographic Procedure. Data was collected on a Nicolet P3 diffractometer at room temperature using Mo Kα radiation with a graphite-crystal monochromator in the incident beam. A 1.2-mm collimator was used, producing a beam with an approximately 1 mm uniform diameter. Fifteen reflections from a rotation photograph were computer-centered, and the resulting setting angles were used in the autoindexing program, in conjuction with axial photographs, to select the best unit cell. Final cell constants were based on 15 reflections collected in a 2θ range of 25–40°. Structure solving was done on a VAX 11/780 computer using the Enraf-Nonius Structure Determination Package of crystallographic programs.

A yellow–green crystal of **6a** measuring 0.42 mm × 0.18 mm × 0.06 mm was mounted with epoxy at the end of a glass fiber. The crystal was found to be orthorhombic with final unit cell dimensions a = 25.506 (4) Å, b = 11.206 (2) Å, c = 15.922 (3) Å, V = 4550 (4) Å³, and Z = 4. A total of 2565 independent reflections were measured by using the ω scan technique in the range of 3° < 2θ < 45° with a fixed scan rate of 1.0°/min and a symmetrical scan range of 1.0° about the average Mo Kα peak position. Three standard reflections measured every 100 data points showed only small, random variations.

The structure was solved in the space group *Pnma* (identified from systematic absences) by using only those 940 reflections with F_o^2 > 3$\sigma(F_o^2)$. The structure was solved by using the direct methods (MULTAN) series of programs. Anisotropic full-matrix least-squares refinement of the non-hydrogen atoms gave discrepancy indexes of R = 0.098 and R_w = 0.116, defined as $R = \sum(|F_o| - |F_c|)/\sum|F_o|$ and $R_w = [\sum w(|F_o| - |F_c|)^2/\sum w|F_o|^2]^{1/2}$, where $w = 1/\sigma(F_o)^2$. The $Co_2(CO)_4(eHTP)^{2+}$ molecule lies on a mirror plane that passes through the cobalt atoms, the CO groups, the methylene carbon atom, and the two phosphorus atoms bonded to it. The $CoCl_4^{2-}$ counterion also lies on a mirror plane.

At this point, several problems were evident: the data-to-parameter ratio was at an unacceptably low value of 4.2 due to the limited data set from the very small crystal used; one of the $Co(CO)_2$ groups had unusually large thermal parameters (approximately 50% larger than the other $Co(CO)_2$ moiety) which indicated that there could be a partial

(10) Georgopoulos, P.; Knapp, G. S. *J. Appl. Crystallogr.* **1981**, *14*, 3.
(11) Merrill, J. J.; Dumond, J. W. M. *Ann. Phys. (N.Y.)* **1961**, *14*, 166.

(12) Bleeke, J. R.; Peng, W.-J. *Organometallics*, in press.
(13) Marques, E. C. Ph.D. Dissertation, Washington State University, 1983.
(14) McMaster, W. H.; del Grande, N. K.; Mallet, J. H.; Hubbel, J. H. *Annu. Rep.—Natl. Bur. Stand. (U. S.)* **1969**, Report No. UCRL-50174, Section II, Review 1.
(15) For a more detailed discussion of the EXAFS technique and the data processing involved, see, for example: Via, G. H.; Sinfelt, J. H.; Lytle, F. W. *J. Chem. Phys.* **1979**, *71*, 690.

7426 *J. Am. Chem. Soc., Vol. 107, No. 25, 1985*

Askham et al.

Table I. Crystallographic Data for Co$_2$(CO)$_4$(eHTP)·2PF$_6$

Crystal Parameters

formula = Co$_2$P$_8$F$_{12}$O$_4$C$_{29}$H$_{58}$	MW = 1064.08
cryst system = monoclinic	space group = $C2/c$
a = 26.464 (4) Å	α = 90.0°
b = 12.562 (2) Å	β = 99.04 (1)°
c = 14.380 (3) Å	γ = 90.0°
V = 4721 (3) Å^3	Z = 4
d_{calcd} = 1.49 g/cm^3	μ(Mo Kα) = 10.46 cm^{-1}
cryst size = 0.68 × 0.35 × 0.33 mm	temp = 22 °C

Data Collection and Structure Refinement

diffractometer = Nicolet P3	radiation = Mo Kα
monochrometer = graphite cryst	scan method = ω
scan speed = variable, 1.0–29.8° min^{-1}	data limits = 3° < 2θ < 55°
reflections collected = 6864	unique data $F_o^2 > 3\sigma(F_o)^2$ = 4059
no. of parameters refined = 251	data/parameter ratio = 16.0
R^a = 0.070	$R_w{}^b$ = 0.106
quality of fit indicator^c = 2.103	largest final Fourier peak = 0.78 e/Å^3
largest shift/esd, final cycle = 0.5	

$^a R = \Sigma||F_o| - |F_c||/\Sigma|F_o|.$ $^b R^w = [\Sigma w(|F_o| - |F_c|)^2/\Sigma w|F_o|^2]^{1/2};$ $w = 1/\sigma(|F_o|).$ ^{c}Quality of fit = $[\Sigma w(|F_o| - |F_c|)^2/(N_{obsd} - N_{parameters})]^{1/2}.$

Table II. Table of Positional Parameters and Their Estimated Standard Deviations^a

atom	x	y	z	$B(A^2)$
Co	0.110 00 (3)	0.189 95 (5)	0.162 44 (4)	4.23 (1)
P1	0.050 68 (5)	0.298 6 (1)	0.195 7 (1)	4.60 (3)
P2	0.086 92 (6)	0.244 8 (2)	0.016 4 (1)	5.78 (3)
P3	0.156 90 (7)	0.255 7(2)	0.289 3 (1)	6.12 (4)
O1	0.200 9 (2)	0.104 9 (6)	0.103 0 (4)	11.2 (2)
O2	0.059 8 (2)	−0.009 4 (4)	0.202 5 (4)	8.6 (1)
C1	0.164 6 (3)	0.138 0 (6)	0.126 3 (5)	7.0 (2)
C2	0.079 5 (2)	0.069 1 (5)	0.186 7 (4)	5.7 (1)
C'	0.000	0.234 0 (6)	0.250	4.3 (1)
C11	0.016 4 (3)	0.362 8 (6)	0.086 4 (5)	7.6 (2)
C12	0.048 8 (3)	0.366 5 (7)	0.013 3 (5)	9.1 (2)
C13	0.079 7 (3)	0.401 1 (5)	0.273 9 (5)	6.8 (2)
C14	0.117 2 (3)	0.349 8 (6)	0.347 5 (5)	7.7 (2)
C21	0.043 4 (4)	0.145 3 (8)	−0.058 9 (6)	10.9 (3)
C22	0.064 3 (4)	0.043 8 (8)	−0.061 6 (7)	10.1 (3)
C23	0.135 3 (4)	0.277 (1)	−0.058 6 (6)	9.9 (3)
C24	0.175 4 (4)	0.352 (1)	−0.021 4 (8)	10.9 (3)
C31	0.213 1 (4)	0.333 2 (9)	0.270 5 (8)	12.9 (3)
C32	0.239 0 (5)	0.385 (1)	0.361 (1)	18.3 (5)
C33	0.174 0 (4)	0.156 5 (8)	0.388 1 (6)	10.8 (3)
C34	0.205 6 (4)	0.071 2 (9)	0.364 6 (7)	11.5 (3)
P4	0.120 24 (8)	0.700 2 (2)	0.137 6 (1)	6.89 (4)
F1	0.165 6 (2)	0.685 2 (5)	0.080 4 (4)	11.8 (2)
F2	0.088 9 ()	0.610 6 (5)	0.081 4 (5)	14.8 (2)
F3	0.092 3 (2)	0.772 0 (5)	0.056 1 (5)	12.7 (2)
F4	0.075 8 (3)	0.725 0 (8)	0.194 0 (5)	15.2 (2)
F5	0.149 0 (3)	0.791 9 (5)	0.190 9 (7)	16.5 (3)
F6	0.143 2 (3)	0.622 7 (6)	0.215 7 (4)	14.8 (2)
O3	0.500	0.104 (1)	0.250	7.0 (3)*

^{a}Starred atoms were refined isotropically. Anisotropically refined atoms are given in the form of the isotropic equivalent thermal parameter defined as $^4/_3$ $[aaB(1,1) + bbB(2,2) + ccB(3,3) + ab(\cos \gamma)$-$B(1,2) + ac(\cos \beta)B(1,3) + bc(\cos \alpha)B(2,3)]$.,

vacancy of the Co(CO)$_2$ positions (larger than normal thermal parameters on the CoCl$_4$$^{2-}$ also supported this observation of incomplete site occupancy); and the Co–CO bond lengths were too short by about 0.10 Å. The eHTP ligand framework, on the other hand, had normal bond distances and angles. We decided, therefore, to look at the structure of the PF$_6^-$ salt, **6b**, from which we had subsequently been able to grow much better crystals. Although we will not present the structural details of **6a** due to the problems outlined above, the basic structure of the Co$_2$(CO)$_4$(eHTP)$^{2+}$ cation is the same as that which is found for **6b**.

A well-formed yellow crystal of **6b** measuring 0.68 mm × 0.35 mm × 0.33 mm was mounted with epoxy on a glass fiber. Crystal and collection data are listed in Table I. ω scan data collection was used because of the 26-Å axis and the relatively large unit cell. During the early part of data collection, there was a 10% variation in the intensity of the standards over a 15-h period that was apparently caused by some sort of power fluctuation. This was corrected for by use of the anisotropic decay correction program CHORT. The space group assignment of $C2/c$ was indicated by statistical tests and by the subsequent successful refinement of the structure in this space group. Refinement in the acentric space group Cc was checked, however, and although the data could be refined in Cc, we obtained poorer discrepancy indexes as well as bond lengths and angles that were very unreasonable.

The structure was solved by using direct methods (MULTAN) and a Patterson map, from which the Co and four P atoms were located. This initial model gave discrepancy indexes of R = 0.48 and R_w = 0.61. This model could not be refined, however, despite strong evidence from the Patterson and Direct Methods results that the cobalt and phosphorus atomic coordinates were correct. Although the cobalt position refined well, the positions of the phosphorus atoms did not; difference Fourier maps were not properly phased and did not reveal any other atom positions. We felt that the difficulties could be the result of a false minimum problem and managed to break the false minimum by applying a 0.20 dampening factor to the parameter shifts in the full-matrix least-squares refinement. After four cycles of refinement, the discrepancy indexes dropped dramatically on the fourth cycle to give R = 0.352 and R_w = 0.473. Subsequent difference Fourier maps revealed the location of all non-hydrogen atoms.

The difference Fourier maps, at this point, revealed the presence of a peak of electron density measuring 2.09 e/Å^3, lying on a 2-fold axis that was well separated from the anion or cation molecules. This was assumed to be, and refined as, a water molecule which comes from the recrystallization solvent system of acetone/ethanol/H$_2$O. The magnitude of electron density indicated only partial occupancy of the site, which was confirmed by the least-squares refinement which gave far too large thermal parameters assuming 100% occupancy. An occupancy of 50% gave reasonable thermal parameters but was not refined.

Anisotropic refinement of all non-hydrogen atoms gave the final discrepancy indexes of R = 0.070 and R_w = 0.106 with a GOF of 2.103. A difference Fourier map at this point revealed the presence of about one-third of the hydrogen atoms. Since we could not locate a majority of the hydrogen atoms, their positions were, therefore, all calculated into place.

The larger-than-usual thermal parameters on the PF$_6^-$ are probably due to a partial disordering of this group which could not be resolved.
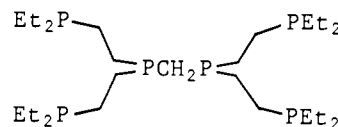
This type of disorder, which generally shows up as larger-than-normal thermal parameters, is quite common for PF$_6^-$ and BF$_4^-$ anions. The somewhat larger thermal parameters for the ethyl groups on the eHTP ligand are not particularly surprising since one would expect the ethyl groups to be quite "floppy", and the pattern of increasing motion as one moves from the methylene to the methyl groups is reflected in the size of the thermal parameters. The unusually large value for C32 may be tied into an unresolvable disorder caused by that ethyl group having two slightly different rotameric conformations. The shorter than normal bond distance for C21–C22 is probably a result of the incompletely resolved false minimum problem.

The discrepancy indexes and GOF indicator are somewhat larger than expected. To a large part, we believe that this can be tied into the power fluctuation during data collection which threw off some of the low angle data. This and the thermal motion of the ethyl groups may be the reason why we were not able to locate and refine the hydrogen atoms. The data from this and other crystals of **6b** were not particularly good, and we had considerable problems with "false minimum"-type solutions showing up mainly in the form of too short C–C bond lengths. We collected four data sets from three different crystals in attempts to resolve this problem with the best of the data sets presented here.

The final positional and isotropic equivalent thermal parameters are listed in Table II. Tables of the anisotropic thermal parameters, hydrogen atom coordinates, structure factors, and a full listing of bond distances and angles are included in supplementary material.
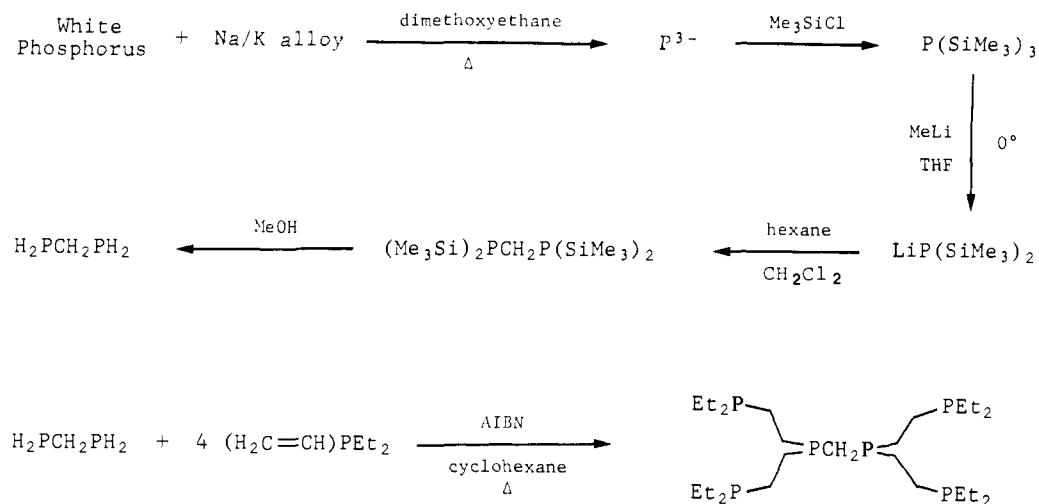
Results and Discussion

Ligand System. The hexa-*tert*-phosphine ligand eHTP, (R$_2$PCH$_2$CH$_2$)$_2$PCH$_2$P(CH$_2$CH$_2$PR$_2$)$_2$, **1** (R = Et), contains a central bis(phosphino)methane bridging group with four ethylene-linked tertiary phosphines, creating a ligand system that can both bridge and tris-chelate two metal centers. This combination
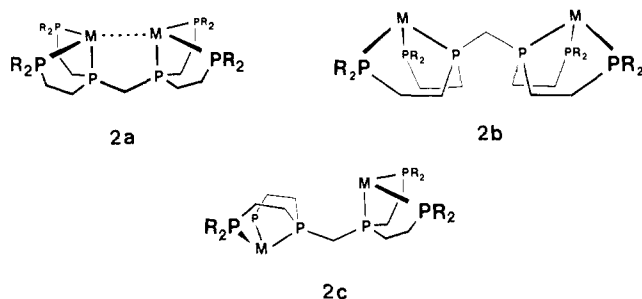

1

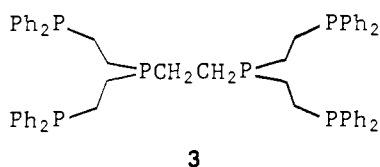of bridging and tris-chelation should make for a flexible, yet rugged

Scheme I

binucleating ligand system that can form closed- and open-mode dimeric species such as **2a**, **2b**, and **2c** (assuming tris-chelation to be a driving coordination factor).

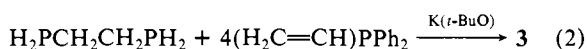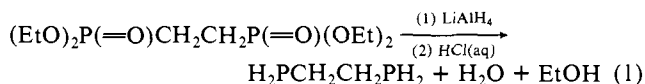**2a**   **2b**

2c

King and co-workers have prepared a similar hexaphosphine ligand, **3**, that has a central ethylene linkage and was designed to act as a hexachelating phosphine analogue of EDTA.[16]
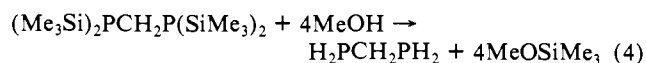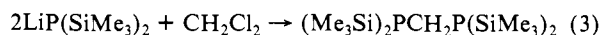

3

Problems with low synthetic yields (<30%), in addition to low ligand and even lower transition-metal complex solubilities, limited the chemistry of **3**.[16] Hexachelation, moreover, was never observed due to the bulky –PPh$_2$ groups which prevented **3** from closing up around a single metal center.

King's synthesis involved the hydride reduction of (RO)$_2$P-(O)CH$_2$CH$_2$P(O)(OR)$_2$ to yield bis(phosphino)ethane (eq 1) followed by base-catalyzed addition of (H$_2$C=CH)PPh$_2$ to yield **3** (eq 2).[16] Unfortunately, the equivalent reaction to give H$_2$P-

$$(EtO)_2P(=O)CH_2CH_2P(=O)(OEt)_2 \xrightarrow[\text{(2) HCl(aq)}]{\text{(1) LiAlH}_4}$$
$$H_2PCH_2CH_2PH_2 + H_2O + EtOH \quad (1)$$

$$H_2PCH_2CH_2PH_2 + 4(H_2C=CH)PPh_2 \xrightarrow{\text{K(t-BuO)}} 3 \quad (2)$$

CH$_2$PH$_2$ from the reduction of (RO)$_2$P(O)CH$_2$P(O)(OR)$_2$ proceeds, at best, in only about 15–19% yields which we considered to be unacceptably low.[17,18]

An alternate route to H$_2$PCH$_2$PH$_2$, however, was provided by the silylphosphine work of Fritz and Holderich shown in eq 3 and 4.[7] The addition of phosphides to dihalomethanes to generate

$$2LiP(SiMe_3)_2 + CH_2Cl_2 \rightarrow (Me_3Si)_2PCH_2P(SiMe_3)_2 \quad (3)$$

$$(Me_3Si)_2PCH_2P(SiMe_3)_2 + 4MeOH \rightarrow$$
$$H_2PCH_2PH_2 + 4MeOSiMe_3 \quad (4)$$

a bis(phosphino)methane type unit turns out to be a rather sensitive reaction. Diphenyl phosphide, for example, will react with dichloromethane to give bis(diphenylphosphino)methane in high yields. PH$_2^-$, on the other hand, undergoes extensive free-radical self-coupling reactions to yield H$_2$PPH$_2$ and coupled organic products.[19] P(SiMe$_3$)$_2^-$ appears to have the proper electronic and steric balance to do a clean substitution on CH$_2$Cl$_2$ to give (Me$_3$Si)$_2$PCH$_2$P(SiMe$_3$)$_2$ in high yields.

Fritz reported an 82% yield on eq 3 which was run in cyclopentane when using the LiP(SiMe$_3$)$_2$·2THF adduct.[7] We have found, however, that removal of excess THF from the LiP(SiMe$_3$)$_2$ by vacuum-drying prior to reaction with CH$_2$Cl$_2$ (our solvent was hexane) increased the yield of (Me$_3$Si)$_2$PCH$_2$P(SiMe$_3$)$_2$ to almost quantitative (isolated yield = 89–94%). Moreover, the reaction of (Me$_3$Si)$_2$PCH$_2$P(SiMe$_3$)$_2$ with MeOH does quantitatively yield H$_2$PCH$_2$PH$_2$.

The overall synthesis for **1** is outlined in Scheme I and is an amalgamation and modification of preparations by Becker,[6] Fritz,[7] and Meek.[20] Although the *overall* isolated yield of **1** is in the 50–60% range, if one starts from P(SiMe$_3$)$_3$, which is synthesized from inexpensive and easily obtained starting materials, the isolated yield is in the 75–85% region.

The ^{31}P NMR of **1** is rather interesting and is shown in Figure 1. The downfield, pseudotriplet pattern is assigned to the four terminal phosphorus atoms and the upfield pattern to the two internal phosphorus atoms. The 9 ppm difference in the chemical shifts of the internal and external phosphorus atoms might appear, at first sight, to be somewhat surprising based on the ^{31}P NMR of other multidentate phosphine ligands. (Ph$_2$PCH$_2$CH$_2$)$_2$PPh, for example, has a classic second-order AB$_2$ ^{31}P NMR spectrum with the two different phosphorus atoms only separated by 3.8 ppm (–12.8 and –16.6 ppm).[21] A very similar second-order ^{31}P

---

(16) King, R. B.; Saran, M. S. *Inorg. Chem.* **1971**, *10*, 1861.
(17) (a) Monsanto Co. Brit. Patent 1 130 487, Oct 1968. (b) *Chem. Abstr.* **1969**, *70*, 37915v.

(18) Very recently there have been several publications reporting higher-yield syntheses of H$_2$PCH$_2$PH$_2$. The reported yields, however, are still only in the 30–40% region. (a) Issleib, K.; Krech, F.; Kuhne, U. *Z. Chem.* **1984**, *24*, 261. (b) Stelzer, O.; Hietkamp, S.; Sommer, H. *Chem. Ber.* **1984**, *117*, 3400.
(19) Stanley, G. G.; Askham, F. R., unpublished results.
(20) Uriarte, R.; Mazanec, T. J.; Tau, K. D.; Meek, D. W. *Inorg. Chem.* **1980**, *19*, 79.
(21) Meek, D. W.; DuBois, D. L.; Tiethof, J. In "Inorganic Compounds with Unusual Properties"; King, R. B., Ed.; ACS: Washington D.C., 1976; ACS Symp. Ser. No. 150, p 335.

NMR with a difference of 2.3 ppm (−17.3 and −19.6 ppm) is also seen for the related ethyl-substituted tris-chelating phosphine, $(Et_2PCH_2CH_2)_2PPh$, which we have prepared to act as a model ligand for comparing the reactivities of mononuclear systems to that of **1**.[19]

Grim, however, has developed an empirical scheme for calculating the chemical shifts of the phosphine ligand based on group contributions which quite accurately predicts the values observed for **1** (predicted/observed: $P_{int} = -20.5/-19.3$ ppm, $P_{ext} = -28/-28.2$ ppm).[22] Grim's group contribution scheme, for example, predicts a 20 ppm difference between the internal ($P_{int} = -28$ ppm) and external ($P_{ext} = -48.5$ ppm) phosphorus atoms in the methyl-substituted analogue of **1**, $(Me_2PCH_2CH_2)_2PCH_2P-(CH_2CH_2PMe_2)_2$, which we are also planning to synthesize.

The spectrum can be interpreted as an $A_2XX'A_2'$-type system with strong two-bond coupling between the chemically equivalent X and X' phosphorus atoms (P1 and P2) and medium three-bond coupling between the A and X atoms (P1–P3, P2–P4). We have used this coupling scheme to successfully simulate the spectrum as shown in Figure 1. There is a somewhat lower-than-normal P1–P3, P2–P4 coupling constant of 21.0 Hz, compared to a typical 3-bond P–P coupling constant of 25–30 Hz.[20,23] In this type of coupling scheme, this coupling constant is given by the peak difference between the two *outside* peaks of the pseudotriplet pattern. The 107.5-Hz coupling between P1–P2 is, however, about what one might expect from previous work on unsymmetrically substitued alkyl- and arylbis(phosphino)methanes.[24]

The simulation also indicates that the P1–P2 and P1–P3 coupling constants have opposite signs. This does not, unfortunately, fit in with previous work on the signs of $^2J_{P-P}$ and $^3J_{P-P}$ coupling constants in simple P(III) diphosphine systems.[25] Since the relative sign change in our system was derived from a simulation and not through more sophisticated NMR techniques such as heteronuclear triple resonance experiments,[25] we cannot be sure of our assignment. This ligand system, however, offers the first example of a P(III) system with both two- and three-bond P–P couplings which one could examine at the same time. More detailed experiments are clearly called for to sort out this perhaps interesting question.

Finally, both the experimental spectrum and the simulation clearly show that the two sets of phosphorus resonances have rather different line widths (1.7 Hz for P1,2 and 2.9 Hz for P3,4). This points to different T_2 times for the phosphorus atoms, with the internal P1,2 atoms having a longer T_2 and, hence, smaller line widths. This is what one would qualitatively expect since the more rotationally hindered internal phosphorus atoms should have longer T_2's.

$Co_2Cl_{4-x}(eHTP)^{x+}$ ($x = 0$ or 2). The reaction of **1** with 2 equiv of $CoCl_2$ in polar solvents, such as THF or ethanol, initially yields a reddish-brown, extremely air-sensitive, paramagnetic product **4**, which on standing deposits a green, air-sensitive, paramagnetic precipitate **5**. Both of these compounds seem to have the same overall empirical formula of $Co_2Cl_4(eHTP)$, where eHTP = **1**.

Since we have been unable to obtain single crystals of either of these paramagnetic complexes, we have decided to make use of Extended X-ray Absorption Fine Structure (EXAFS) spectroscopy to give us information about the nature of these products. EXAFS spectra can give information about the oxidation state of the metal, number, and type of atoms in the immediate coordination sphere and distances from the metal to the ligands.[15] The availability of a laboratory EXAFS spectrometer in the Physical Sciences Center at Monsanto allows us to make ready use of the EXAFS technique to determine whether our eHTP complexes are in an open- or closed-mode configuration and what the M–M contact distance is in the case of a closed geometry.
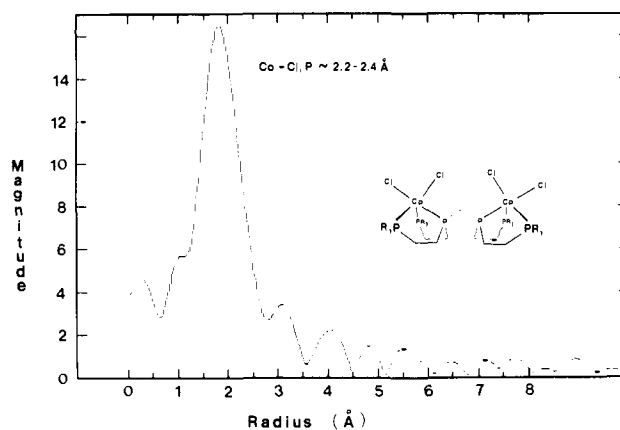

Figure 2. Fourier transformed Extended X-Ray Absorption Fine Structure (EXAFS) spectrum of $Co_2Cl_4(eHTP)$, **4**. The spectrum shows the non-phase-shifted radial distribution of ligand bond distances about the cobalt atom. The scattering factor phase shift corrected bond distances are listed by the peak.

On the basis of the position of the Co X-ray absorption edge, the EXAFS spectra of both **4** and **5** indicate that the cobalt atoms are in the +2 oxidation state. The radial distribution of Co–ligand distances from the Fourier transform of the EXAFS data, shown in Figure 2, clearly shows that **4** has a strong contact at the uncorrected distance of 1.8 Å. Assuming that this results from Co–P- and Co–Cl-type bonds, one can apply the scattering factor phase-shift correction[15] of +0.5 Å for phosphorus and chlorine atoms to obtain Co–P and Co–Cl bond distances in the 2.3-Å region. The width of the peak, furthermore, points to a range in bond distances from about 2.2 to 2.4 Å. This result agrees well with a crystal structure on $CoCl_2(PMe_3)_3$ which has Co–P bond distances of 2.24 (3), 2.24 (3), and 2.25 (3) Å and Co–Cl bond distances of 2.26 (3) and 2.34 (4) Å.[26a]

If the complex was in a closed-mode configuration, one would expect a Co–Co contact distance in the 2.5–3.2-Å region. Since a cobalt atom has an EXAFS scattering factor phase shift of about +0.3 Å, one would, therefore, expect a sizable peak due to the Co⋯Co vector to occur in the EXAFS spectrum between 2.2 and 2.9 Å. As no such peak is seen in this area of the spectrum, we conclude that **4** has an open-mode geometry.

Although we could have taken the data analysis further to determine the number of ligands about the cobalt atom, the crude data were sufficient to tell us whether the complex was in an open- or closed-mode configuration and to give us a good estimate of the Co–P and Co–Cl bond distances. Based on this information, and the nature of the eHTP ligand system, we propose that **4** is an open-mode Co(II) complex with approximate trigonal-bipyramidal geometry about each cobalt atom (three phosphorus and two chloride ligands). This is quite consistent with the known chemistry of other mononuclear Co(II) phosphine/halide complexes.[26]

Our choice of open-mode-type **2b** over **2c** for the structure of **4** is based on a qualitative examination of steric effects for five-coordinate metals in these two possible eHTP open-coordination modes. Both space-filling models and the CHEMGRAF molecular graphics program[27] indicate that for a five-coordinate metal, such as we have proposed for **4**, mode **2b** is definitely the preferred conformation. The crystal structure of the related complex, $Co_2(CO)_4(eHTP)^{2+}$, discussed below also has this type of structure, which further supports the proposed ligand conformation in **4**.

(22) (a) Grim, S. O., personal communication. (b) Grim, S. O.; McFarlane, W.; Davidoff, E. F. *J. Org. Chem.* **1967**, *32*, 781.

(23) Grim, S. O.; Del Gaudio, J.; Molenda, R. P.; Tolman, C. A.; Jesson, J. P. *J. Am. Chem. Soc.* **1974**, *96*, 3416.

(24) Grim, S. O.; Mitchell, J. D. *Inorg. Chem.* **1977**, *16*, 1770.

(25) Colquhoun, I. J.; McFarlane, W. *J. Chem. Soc., Dalton Trans.* **1982**, 1915.

(26) For $CoX_2(PR_3)_3$ complexes, cf.: (a) Alnagi, O.; Zinoune, M.; Gleizes, A.; Dartiguenave, M.; Dartiguenave, Y. *Nouv. J. Chim.* **1980**, *4*, 707. (b) King, R. B.; Kapoor, P. N.; Kapoor, R. N. *Inorg. Chem.* **1971**, *10*, 1841. (c) Rigo, P.; Bressan, M.; Turco, A. *Ibid.* **1968**, *7*, 1460. (d) Bertrand, J. A.; Plymale, D. L. *Ibid.* **1966**, *5*, 879.

(27) (a) Davies, E. K. "CHEMGRAF Program Suite"; Chemical Crystallography Laboratory, University of Oxford: England, 1982. (b) Newsam, J. M.; Halbert, T. R. *Inorg. Chem.* **1985**, *24*, 491.
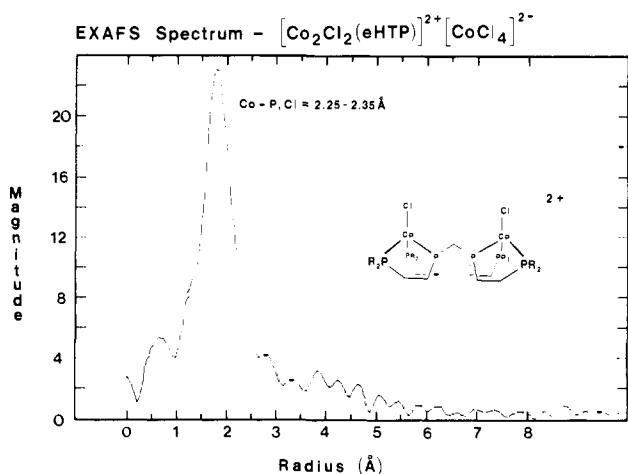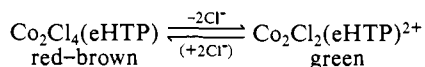
EXAFS Spectrum − $[Co_2Cl_2(eHTP)]^{2+}[CoCl_4]^{2-}$

Figure 3. Fourier transformed EXAFS spectrum of $Co_2Cl_2(eHTP)^{2+}$, **5**. The spectrum shows the non-phase-shifted radial distribution of ligand bond distances about the cobalt atom. The scattering factor phase shift corrected bond distances are listed by the peak.

The conversion of **4** to **5** most probably involves the dissociation of two chloride ligands to generate a tetrahedral, dicationic, Co(II) binuclear complex, which precipitates out of solution, either as the chloride salt or, if an extra equivalent of $CoCl_2$ is used, the $CoCl_4^{2-}$ salt. The EXAFS spectrum of **5** (Figure 3) is very similar

$$Co_2Cl_4(eHTP) \underset{(+2Cl^-)}{\overset{-2Cl^-}{\rightleftharpoons}} Co_2Cl_2(eHTP)^{2+}$$
$$\text{red-brown} \qquad\qquad\qquad \text{green}$$

to that of **4** and shows only a single peak around 1.78 Å, which corresponds to Co–P,Cl bond distances of about 2.25–2.35 Å. The peak is narrower than the one seen in the EXAFS spectrum of **4**, pointing to a more uniform set of Co–P,Cl bond distances. Once again, no peak is seen in the 2.0–4.0-Å region, indicating that **5** is in an open-mode geometry similar to that proposed for **4**.

The dissocation of a chloride from each cobalt atom in **4** to form **5** is, somewhat surprisingly, a rather unusual process. $CoCl_2$ readily reacts with most phosphines (uni- or multidentate) to give four-coordinate tetrahedral $CoCl_2(PR_3)_2$ and five-coordinate (trigonal-bipyramidal or square-pyramidal) $CoCl_2(PR_3)_3$- or $CoCl(PR_3)_4^+$-type complexes. Although a $CoCl(PR_3)_3^+$ species has been proposed in $CoCl(PR_3)_4^+ \rightleftharpoons CoCl(PR_3)_3^+ + PR_3$ equilibrium studies,[26a] there turns out to be only one $CoCl(PR_3)_3^+$ complex that has been characterized so far, $CoCl(Pom-P-Pom)^+$ (where Pom-P-Pom = $((MeO)_2PCH_2CH_2)_2PR$, and R = Ph or Me).[28]

The colors of **4** and **5**, compared to other known Co(II) chloro/phosphine complexes, seem to fit in well with their proposed formulations as five-coordinate, trigonal-bipyramidal, and four-coordinate tetrahedral complexes. $CoCl_2(etp)$ (etp = $(Ph_2PCH_2CH_2)_2PPh)$), for example, is an orange–red compound with trigonal-bipyramidal geometry,[26b] while $CoCl(Pom-P-Pom)^+$ is a green complex with tetrahedral geometry.[28] The eHTP ligand apparently has the proper electronic factors to allow access to both types of complexes.
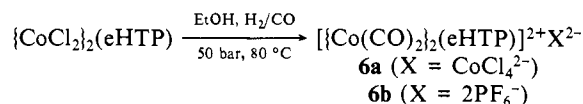
There appears to be an equilibrium set up between **4** and **5**, with **4** as the preferred species. The insolubility of **5** in the solvents we ran the reaction in, however, pushes the equilibrium in the direction of **5**. Dissolving **5** in oxygen-free H_2O instantly regenerates the red–brown solution of **4** by releasing Cl⁻ tied up in the $CoCl_4^{2-}$ counteranion and allowing the equilibrium, which favors **4**, to reestablish itself.

Considering the EXAFS spectrum, colors, and the solution data, we propose that the structure of **5** is open-mode (type **2b**) with tetrahedral geometry about each cobalt atom. Although open-mode **2c** is also feasible for a tetrahedral metal based on space-filling models and the CHEMGRAF van der Waals' energy calculations, the ease with which **5** is converted back to **4** causes us

4   5

to favor the same eHTP conformation for both species.

$Co_2(CO)_4(eHTP)^{2+}$ Synthesis. Reaction of *either* of the two $Co_2Cl_4(eHTP)$ complexes (alone or mixed) with an extra equivalent of $CoCl_2$ and H_2/CO gives, in high yields (>95%), the moderately air-stable, yellow–green Co(I) dimer complex $[Co_2(CO)_4(eHTP)]^{2+}[CoCl_4]^{2-}$, **6a**. Aqueous metathesis with $NaPF_6$

$${CoCl_2}_2(eHTP) \xrightarrow[\text{50 bar, 80 °C}]{\text{EtOH, } H_2/CO} [\{Co(CO)_2\}_2(eHTP)]^{2+}X^{2-}$$
$$\text{6a } (X = CoCl_4^{2-})$$
$$\text{6b } (X = 2PF_6^-)$$
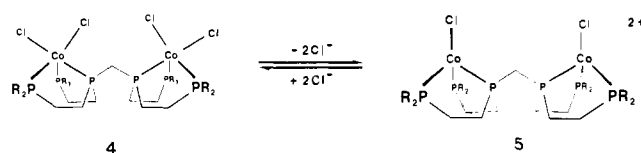
gives the yellow PF_6^- salt, **6b**, which can be recrystallized by slow evaporation of an ethanol/acetone/H_2O mixture.

The formation of **6** is easily understood in terms of previous work by Meek and co-workers on the synthesis of the monomeric complex $Co(CO)_2(P_3)^+$, where P_3 can be the tris-chelating phosphine ligands $PhP(CH_2CH_2PPh_2)_2$, (etp), or $PhP(CH_2CH_2CH_2PPh_2)_2$, (ttp).[29–31] $Co(CO)_2(P_3)^+$ is, to a very good approximation, half of our complex, and their chemistries are quite parallel. Reaction of P_3 with $CoCl_2$, for example, gives $CoCl_2(P_3)$ which can then be reduced with $NaBH_4$ under CO to yield $CoH(CO)(P_3)$. Subsequent reaction of $CoH(CO)(P_3)$ with acids under an atmosphere of CO produces $Co(CO)_2(P_3)^+$.

We accomplish the same thing, in a single step, by using an H_2/CO mixture. We propose that H_2 reduces ${CoCl_2}_2(eHTP)$ to ${CoH(CO)}_2(eHTP)$, releasing HCl, which can, in turn, reattack to give ${Co(CO)_2}_2(eHTP)^{2+}$. The extra $CoCl_2$ that is added reacts with some of the excess Cl⁻ to give the $CoCl_4^{2-}$ counteranion. The CO infrared stretching frequencies of **6b** (2019, 1968 cm⁻¹, KBr) are quite similar to those seen in Meek's monomeric $Co(CO)_2(etp)^+$ complex (2020, 1980 cm⁻¹, Nujol).

Interestingly, if an extra equivalent of $CoCl_2$ is not added, one still forms ${Co(CO)_2}_2(eHTP)^{2+}CoCl_4^{2-}$, **6a**, only in lower yields. The monometallic complex, $Co(CO)_2(eHTP)^+$, is also produced which cocrystallizes with **6a**, giving rise to the partial occupancies we observed in the structure of **6a** (see Experimental Section). Apparently, in the early stages of the reduction, the HCl released can attack a molecule of ${CoCl_2}_2(eHTP)$, ripping off $CoCl_4^{2-}$ and leaving behind the mononuclear Co(II) complex, $CoCl_2(eHTP)$. This can, in turn, be reduced to a Co(I) carbonyl hydride and protonated to give $Co(CO)_2(eHTP)^+$.

Structure of $Co_2(CO)_4(eHTP)^{2+}$. The infrared spectrum of **6** indicates only two terminal CO bands that are at very similar positions to those seen in $Co(CO)_2(etp)^+$.[21] The ³¹P NMR of **6** is a quadrapole-broadened quintet pattern (1 P) at 127.2 ppm and a doublet (2 P) at 83.4 ppm (referenced to H_3PO_4). The large downfield shift of the internal phosphorus atoms, in contrast to the ordering seen for the free ligand, is a result of the fact that the internal phosphorus atoms are involved in two five-membered chelate rings, while the external phosphorus atoms are involved in only a single chelate ring.[32] The spectral data point to an open-mode structure with the same type of trigonal-bipyramidal structure that Meek proposed for $Co(CO)_2(etp)^+$, with one carbonyl ligand in an equatorial position.[30,31] The EXAFS spectrum of **6a** is shown in Figure 4 and clearly shows peaks corresponding to the Co–CO and Co–P,Cl ligands ($CoCl_4^{2-}$ is present in **6a**). As in **4**, no Co–Co vector is seen between 2.0 and 4.0 Å, indicating that **6** is in an open-mode geometry similar to **4**.

The crystal structure of **6b** (Figures 5 and 6) confirms that the ligand is in the expected open-mode ligand conformation of type

---

(28) King, R. B.; Bibber, J. W. *Inorg. Chim. Acta* **1982**, *59*, 197.

(29) Dubois, D. L.; Meek, D. W. *Inorg. Chim. Acta* **1976**, *19*, L29.
(30) Dubois, D. L.; Meek, D. W. *Inorg. Chem.* **1976**, *15*, 3076.
(31) Mason, R.; Scollary, G. R.; Dubois, D. L.; Meek, D. W. *J. Organomet. Chem.* **1976**, *114*, C30.
(32) (a) Garrou, P. E. *Chem. Rev.* **1981**, *81*, 229. (b) Grim, S. O.; Barth, R. C.; Mitchell, J. D.; DelGaudio, J. *Inorg. Chem.* **1977**, *16*, 1776.
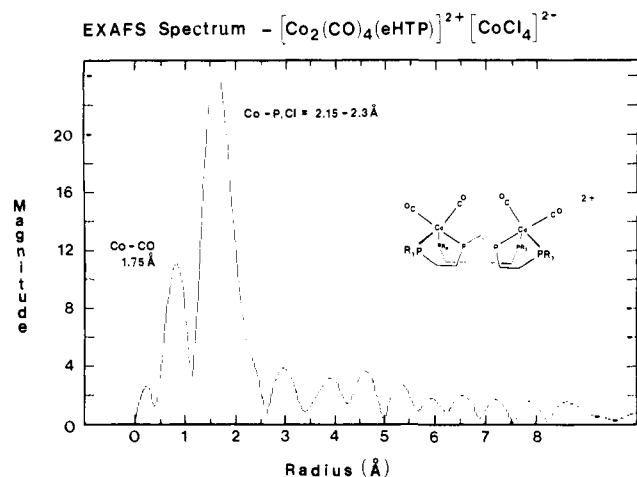
EXAFS Spectrum $-\left[Co_2(CO)_4(eHTP)\right]^{2+}\left[CoCl_4\right]^{2-}$

Figure 4. Fourier transformed EXAFS spectrum of $Co_2(CO)_4$-$(eHTP)^{2+}\cdot CoCl_4^{2-}$, **6a**. The spectrum shows the non-phase-shifted radial distribution of ligand bond distances about the cobalt atom. The scattering factor phase shift corrected bond distances are listed by the peaks.
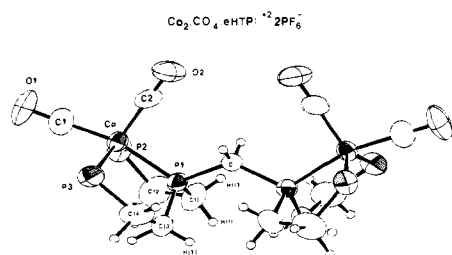
$Co_2CO_4 eHTP^{+2}2PF_6^-$

Figure 5. ORTEP plot of $Co_2(CO)_4(eHTP)^{2+}\cdot 2PF_6^-$, **6b**. The molecule sits on a 2-fold axis that passes through the bridging methylene group. The ethyl groups on P2 and P3 have been omitted for clarity. Thermal elipsoids are drawn at the 33% probability level. All hydrogens shown have been calculated into position and are shown with arbitrarily small thermal elipsoids. The PF_6^- groups are not shown.
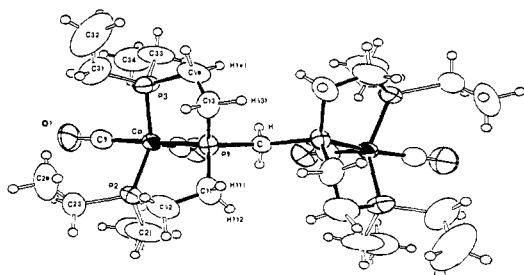
Figure 6. ORTEP plot of $Co_2(CO)_4(eHTP)^{2+}$, **6b**, showing the full molecule. The view is a 90° rotation along the Co⋯Co vector from Figure 5, looking at the "bottom" of the complex.

2b. The molecule sits on a 2-fold rotation axis that passes through the bridging methylene carbon C′. The coordination geometry about each cobalt atom is a distorted trigonal-bipyramid with P2, P3, and C2, defining the equatorial ligand set. The distortion from ideal trigonal-bipyramidal is rather substantial, leaning toward square-pyramidal-type geometry, with equatorial angles for P2–Co–P3 = 135.1 (1)°, P2,3–Co–C2 = 112.8 (1)°, and an axial angle for P1–Co–C1 = 163.3 (2)°. A set of bond distances and angles for **6b** is summarized in Table III. We do not yet completely understand the geometrical coordination preferences of eHTP, since this is the first crystallographically characterized eHTP complex. At least part of this distortion can be attributed to crystal packing forces based on the partial structure of **6a** which showed nearly ideal trigonal-bipyramidal geometry about the two cobalt atoms.

The Co–P distances of 2.18–2.20 Å and Co–CO distances of 1.739 (4) and 1.780 (4) Å in our complex compare quite favorably to those seen in $Co(CO)(P(OMe)_3)(ttp)^+$, where the cobalt geometry is square-pyramidal: Co–P = 2.22–2.23 Å, Co–P(OMe)$_3$

Table III. Selected Bond Distances (in Angstroms) and Bond Angles (in Degrees)[a]

Distances	
Co–P1 = 2.189 (1)	P2–C21 = 1.916 (7)
Co–P2 = 2.203 (1)	P2–C23 = 1.845 (7)
Co–P3 = 2.200 (1)	P3–C14 = 1.865 (5)
Co–C1 = 1.739 (4)	P3–C31 = 1.833 (6)
Co–C2 = 1.780 (4)	P3–C33 = 1.891 (6)
P1–C′ = 1.843 (2)	O1–C1 = 1.143 (5)
C1–C11 = 1.870 (4)	O2–C2 = 1.154 (5)
P1–C13 = 1.800 (4)	C11–C12 = 1.458 (7)
P2–C12 = 1.828 (5)	C13–C14 = 1.480 (7)
intramolecular contacts	
Co–Co = 6.697 (1)	O2–O2 = 3.638 (8)
H111–H131′ = 2.30	

Angles	
P1–Co–P2 = 84.95 (4)	C′–P1–C11 = 104.9 (2)
P1–Co–P3 = 85.14 (4)	C′–P1–C13 = 108.5 (2)
P1–Co–C1 = 163.3 (2)	C11–P1–C13 = 108.7 (3)
P1–Co–C2 = 97.2 (1)	Co–P2–C12 = 110.8 (2)
P2–Co–P3 = 135.11 (5)	P1–C11–C12 = 110.9 (3)
P2–Co–C1 = 87.2 (2)	P2–C12–C11 = 109.9 (4)
P2–Co–C2 = 112.8 (1)	P1–C13–C14 = 107.9 (3)
P3–Co–C1 = 90.1 (2)	P3–C14–C13 = 108.5 (3)
P3–Co–C2 = 111.8 (1)	Co–P3–C14 = 109.0 (2)
C1–Co–C2 = 99.4 (2)	P1–C′–P1 = 127.7 (3)
Co–P1–C′ = 114.4 (1)	Co–C1–O1 = 179.1 (5)
Co–P1–C11 = 110.8 (2)	Co–C2–O2 = 180.0 (5)
Co–P1–C13 = 109.4 (1)	

[a] Numbers in parentheses are estimated standard deviations in the least significant digits.

= 2.19 Å, and Co–CO = 1.729 Å.[30] It is interesting to note that the axial carbonyl, C(1)–O(1), in our structure has the shorter of the two Co–CO bond distances, i.e., 1.739 (4) vs. 1.780 (4) Å. In a trigonal-bipyramidal complex, the equatorial position should be the more electron rich coordination site, and one would have expected the carbonyl ligand to have the shorter Co–CO bond distance due to enhanced π backbonding. We are not sure why this bond distance reversal occurs and will resist offering any speculations on this matter at the present time.

This is the first characterized complex that has an "inverted" geometry for a bridging bis(phosphino)methane moiety. Until now, the only bridging coordination mode that has been seen for $R_2PCH_2PR_2$ ligands has been of type **7** (with or without M–M bonding). With bulky R groups, such as phenyls, the $R_2PCH_2PR_2$

7

8
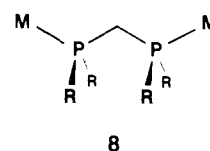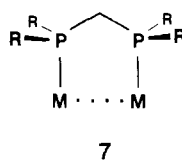
ligand could not possibly form a coordination complex of type **8**. Although the $-CH_2CH_2PEt_2$ arms on eHTP would normally qualify as bulky substituents, the chelation of these groups to the cobalt atoms makes the R groups sterically less bulky and allows the ligand to adopt this unique geometry. The Co⋯Co distance in this open-mode configuration is 6.697 (1) Å, making this the longest M–M distance yet observed for a bis(phosphino)-methane-bridged binuclear system.

An interesting feature of the structure is the unusually large angle about the bridging methylene group (P1–C′–P1) of 127.7 (3)°. This is quite a bit larger than the usual range of 110°–116° seen for $R_2PCH_2PR_2$ dimer complexes.[33] Even in $Pt_2Me_4(dppm)_2$ (dppm = $Ph_2PCH_2PPh_2$), where the two platinum atoms are 4.361 (2) Å apart, the P–CH$_2$–P angles are still only in the 117–119° range.[33a] Mislow and co-workers have reported the largest

(33) (a) Manojlovic-Muir, L.; Muir, K. W.; Frew, A. A.; Ling, S. S. M.; Thomson, M. A.; Puddephatt, R. J. *Organometallics* **1984**, *3*, 1637. (b) Kubiak, C. P.; Eisenberg, R. *Inorg. Chem.* **1980**, *19*, 2726. (c) Kubiak, C. P.; Woodcock, C.; Eisenberg, R. *Ibid.* **1980**, *19*, 2733. (d) Cowie, M.; Dwight, S. K. *Ibid.* **1980**, *19*, 2500. (e) Cowie, M.; Dwight, S. K. *Ibid.* **1979**, *18*, 2700.
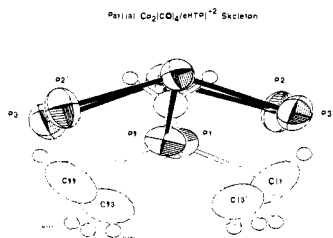
New Type of Transition-Metal Dimer

J. Am. Chem. Soc., Vol. 107, No. 25, 1985 7431

Figure 7. ORTEP plot of the partial skeleton of $Co_2(CO)_4(eHTP)^{2+}$ looking down the Co···Co axis. Carbonyl ligands, ethyl groups, and C12 and C14 of the bridging ethylene groups have been omitted for clarity to show the twisting of the lower half of the complex to avoid steric interactions between C11–C13′ and C13–C11′.

methylene bridge angle so far with a value of 129.3° in bis(9-triptycyl)methane, **9**, which has a C–CH$_2$–C type bridge.[34] As

9
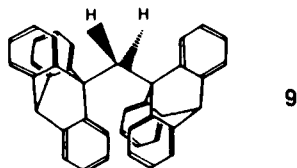
in bis(9-triptycyl)methane, the unusually large angle about the methylene bridge is the direct result of considerable steric interactions that occur, in our complexes, between the ethylene groups on each half of the eHTP ligand that link P1 to P2 and P3. The closest contact distance for the hydrogens on C11 and C13 with those on the 2-fold related groups is 2.30 Å for H111′–H131 and H111–H131′ in their calculated positions. This is within the van der Waals' contact distance of 2.4 Å for hydrogens on different groups, confirming that the considerable steric interaction indicated by the large P1–C′–P1 angle is indeed taking place.

One might expect the eHTP ligand to twist somewhat to relieve these close H···H contact distances. This does happen and is shown in Figure 7 which is an end-on view of the complex looking down the Co···Co vector. The carbonyl ligands, ethyl substituents, and the C12 and C14 atoms in the bridging ethylene groups have been omitted to simplify the view. The dihedral angle between the

planes defined by C11′–P1′–P1 and P1′–P1–C13 is 20°. As can be seen in Figure 7, however, this twist does not extend to the coordination environment about the cobalt atoms. P2′ and P3 are essentially eclipsed with a P2′–Co′–Co/Co′–Co–P3 angle of 4°. Similarly, the angle between the planes defined by the cobalt atom and the two carbonyl ligands with the symmetry-related half is only 4°, indicating once again very little twisting of the upper half of the molecule.

The steric strain involved in the ligand coordination mode **2b** would seem to indicate the potential for the relatively facile conversion to the closed-mode form **2a** upon removal of one, or more, of the carbonyl groups.[35] We are currently probing this possibility by studying reactions of **6b** with Me_3NO or via reduction to Co(0) or Co(−1). Studies of the binuclear complexes of eHTP, as well as the methyl-substituted version, mHTP, with other transition metal systems are also in progress and will be reported in upcoming papers.

Supplementary Material Available: The IR and ^1H NMR of **1** and EXAFS spectrum of **5** as well as listings of thermal parameters, hydrogen atom coordinates, full bond length and angle listings, observed and calculated structure factors for **6b**, figures of the IR and ^1H and ^{31}P NMR spectra of **6b** (26 pages). Ordering information is given on any current masthead page.

(34) Johnson, C. A.; Guenzi, M.; Nachbar, R. B., Jr.; Blount, J. F.; Wennerstrom, O.; Mislow, K. *J. Am. Chem. Soc.* **1982**, *104*, 5163.

(35) We believe that $Co_2Cl_2(eHTP)^{2+}$, **5**, does not close up because of the unfavorable electrostatic effects of placing two Co^+ cations next to one another. Co(II) complexes, particularly cationic ones, have a negligible tendency to form Co–Co bonds, and without some type of M–M bonding interaction to overcome the electrostatic effects, the complex does not want to flip into a closed-mode geometry.